International Journal of Applied Science and Engineering
2004. 2, 3: 257-276

Nonlinear Positioning Compensator of a Novel Thin-Disc Ultrasonic Motor Using Fuzzy Sliding-Mode Control

Chi-Yung Yen[a,b*] , Fuh-Liang Wen[c], and Minsun Ouyang[a]

[a] *Department of Engineering and System Science, National Tsing-Hua University, Hsinchu 300, Taiwan, R.O.C.*

[b] *Department of Electrical Engineering, National United University, Miaoli 360, Taiwan, R.O.C.*

[c] *Department of Mechanical Engineering, St. John's and St. Mary's Institute of Technology, Taipei 251, Taiwan, R.O.C.*

Abstract: An approach of controller design based on fuzzy set and sliding-mode control theory for positioning purpose of a thin-disc edge-driving ultrasonic motor (USM) is developed in this study. A commercially available thin-disc buzzer used as a novel actuating component of ultrasonic motor with simple structure has been demonstrated its cost effectiveness and advantage in flexible mechanism design of a stator and rotor separately according to the necessary of applications. The driving mechanism associated with the non-linear phenomena such as dead-zone and hysteresis behaviors were studied too. Through system identification technique, the approximated transfer function of ultrasonic motor was obtained for controller design using fuzzy sliding-mode (FSMC). It has been successfully applied to position tracking to prove the excellent robust performance in noise rejection.

Keywords: ultrasonic motor; non-linear; dead-zone; hysteresis; fuzzy sliding-mode; robust.

1. Introduction

For decades, the accuracy and affordability of ultrasonic motors (USM) was limited by the mechanical design and piezoelectric material. Ultrasonic motors or actuators were made of piezoelectric bulky material or piezoelectric stacked disks. Their cost was so high that the commercial ultrasonic motor is quite expensive. But, in this study the thin-disc piezoceramic (PZT) has been used for an ultrasonic actuator as an exciting source after conducted a high frequency AC power.

Thus, the novel configuration of thin-disc PZT driving ultrasonic actuator and sliding-mode control technology were employed

* Corresponding author; e-mail: bill@nuu.edu.tw
Accepted for Publication: Sept. 02, 2004

as a key method for going beyond such limitations. The design and performance evaluation of a thin-disc structure ultrasonic actuator has been discussed in Wen et al. [1, 2]. The thin-disc actuator applies mechanically vibrating motion of metal sheet to transfer energy in wave-liking form. The piezoceramic can be operated in an ultrasonic frequency with the amplitude of several micrometers, which is controllable by input voltages.

Consequently, the new approach of ultrasonic actuator is very suitable as a driving device for a compact structure or system and has been patented [3]. Assuming a stable structure is available, how the mechanism can be designed with high kinematical precision might be the next concern. The ultrasonic friction drive exhibits a stick-slip behavior, particularly during the start-up phase.

This phenomenon may be closely related to positioning errors. The USM design is based upon the rotor gear rotated with an ultrasonic friction. This is the main reason why the non-linear problem in contact phenomena should not be ignored. It is also an important issue about driving a loading platform without the influence of both driving errors in a mechanism and the interaction between the rotor and the actuator. However, several other mechanical phenomena that influence the positioning ability are still quite difficult to model precisely. Hysteresis is one of these concerns, for which several attempts were made for suppressing the non-linear properties of the thin-disc USM [4-9].

Some of them are unknown, such as piezoelectric non-linearity. The purpose in this study was to get specialized knowledge and experience to over come the non-linear properties of thin-disc structure in mechanical design. Ever-higher positioning performance is always required because of the needs of micro Electrical Discharge Machining (micro-EDM), for example, of optoelectronic storage devices (DVD tracking and loader).

Therefore, an efficient controller design for USM operation should be performed to minimize the variation of dynamic behaviors and disturbances of the whole system.

Fuzzy sliding-mode control (FSMC) will compensate automatically and dynamically for the effect of un-modeled stick-slip behaviors, and hysteresis on the accuracy of the positioning. In the past decades, sliding-mode control scheme has been successfully applied to various systems such as robot manipulators [10, 11], servo-motors [12-14]. If system perturbations (such as parameter uncertainties and external disturbances) were categorized as the matching type perturbations, the system response would be completely insensitive to those perturbations while in the sliding mode.

Thus, a robust performance can be guaranteed. Hence, the mechanical hysteresis phenomenon of rotation between rotor and stator in clockwise and counterclockwise directions, and nonlinear kinematical interference from slip-stick transmission in frictional contact must be considered as the system parameter of position tracking for the ultrasonic motor.

And, the linear increase of position error is obviously continually multiplied. The position trajectory of the USM looks like a raised circles with identical pitches. Therefore, the advanced modern control strategy of FSMC design for positioning becomes clear. The goal of FSMC control is to stabilize and deescalate the unwanted slope, and to compact raised circles to confine the hysteresis phenomena in kinetic transfer of the PZT thin-disc USM.

This paper first introduces some aspects relating to the position tracking troublesome of controller development for the thin-disc ultrasonic motor. Next section describes the driving circuit of the ultrasonic actuator to give an understanding of the purpose of frequency switching in order to develop the various rotary directions by frequency control in a single-phase AC power input. With operating frequency via system identification technique, an approximated mathematical model was obtained for the controller design.

Due to the existence of non-linearity on thin-disc structure, two types of controller design have been compared in the following section of this paper: sliding-mode control (SMC) and fuzzy sliding-mode control (FSMC).

The last section of this paper, which is based on the analysis of experimental results, discusses the improvement and compensation for nonlinear behaviors using the FSMC structure proposed for the position tracking.

2. Actuating principle and nonlinear dynamic behaviors of USM

This study is related to an ultrasonic motor (USM) using piezoceramic (PZT) driving element, wherein a main sliver electrode is covered at the lowest end of the PZT and the uppermost end of PZT is adhered to a metal sheet, with its dimension specification as shown in Figure 1a. The USM was constructed with a mechanical fixture. An aluminum platform sat atop the rotor shaft in a stationary position by using two ball bearings.

The prototype of the thin-disc PZT driving USM and testing platform is illustrated as Figure 1b. The rotor gear is rotated with an ultrasonic friction actuator. This is the main reason why the non-linear phenomena in friction contact should not be ignored. During operation, a high frequency AC power is activated between the main electrode and the metal sheet. PZT will generate oscillating motion due to the converse piezoelectric effect, and a metal sheet is driven to vibrate in the air to emit sound waves, original operating frequency at sonic frequency. Nevertheless, in this study, this PZT driving element is used as an actuator, operating frequency launched over 30 kHz.

Thus, the generated flexural waves on the metal sheet are transferred along radial or transverse directions. Normally, the diameter of the screw is 2 mm, and to assure the reflection of the waves on the metal sheet, the screw constraint must be locked tightly. The flexural waves from different directions were generated on the metal sheet at its outer edge by setting three reflecting points. The three peripheral constraints were pitched at 90°, 120°, 150° angles respectively, as shown in Figure 2a. Thus, driving mechanism of the vibration mode for the PZT thin-disc USM was constructed [1, 2].

ANSYS simulations, shown in Figure 2, were conducted at 90° arc edge region. The deformation vectors indicated different directions in both of radial (R) and transverse (θ) components when the voltage frequencies of 67 kHz and 75 kHz were individually input.

The variation of the deformation was noted to be enlarged with the higher voltage. When a rotor is tightly against the driving point, as the frequency is at 67 kHz, the rotor will be driven to rotate counterclockwise (θ_R); as the frequency is at 75 kHz, the rotor will move in clockwise direction (θ_F). Thus, edge contact of 90°arc region turned the rotor in clockwise and counterclockwise (respectively) via metal sheet deflection. According to the actuating principle, the proposed thin-disc structure is classified into the quasi-hybrid one, in which one standing wave is the propelling source merged functional reflection waves or deflection waves.

In previous issues, this kind of hybrid USM is a vibrating-rotation-mode USM.

2.1. Hysteresis phenomenon of rotary in (counter-) clockwise

Generally, a valuable edge-driving USM, in a control point of view, shall offer the equilibrium turning torque in clockwise and counterclockwise directions. However, it is hard to be done based on the past trials to gain the consistent torque in both turning directions. According to ANSYS simulations of these screw constraints in PZT thin-disc structure was not only easily investigated, but also directly found the drawback of thin-disc USM in mechanical design in which applied

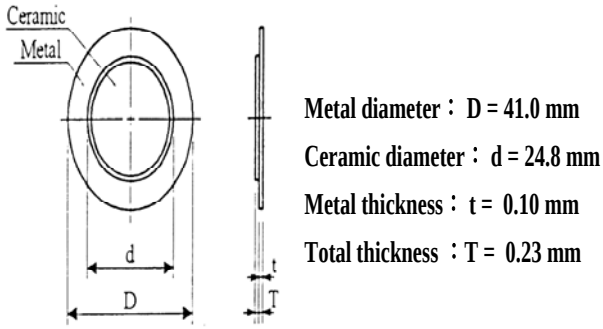

(a)

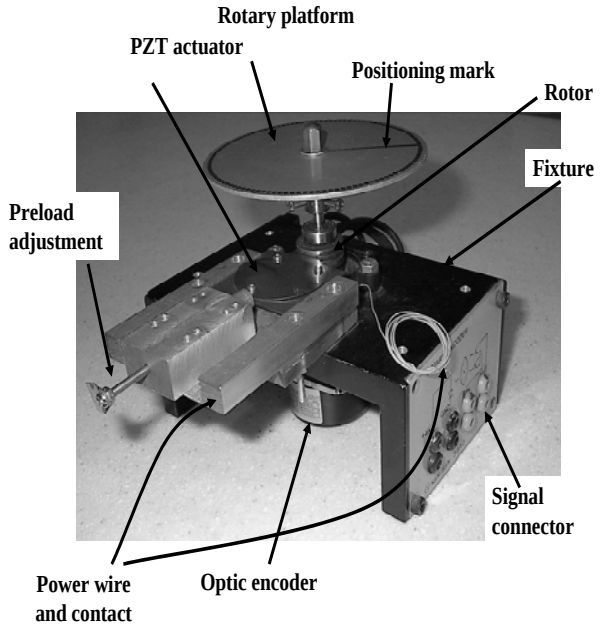

(b)

Figure 1. Ultrasonic component (a) dimensions of thin-disk piezoceramic buzzer and (b) prototype of thin-disk edge-driving type ultrasonic motor

extended-shrunk vibration of metal sheet. From the comparison of Figure 2b and Figure 2c, the combination deflection of 75 kHz in R and θ components is greater than that of 67 kHz. That means the output torque of 75 kHz is larger than that of 67 kHz.

In addition, the efficient deformation at 67 kHz is less than that at 75 kHz. Efficient deformation is defined as the deflection amount of the metal sheet for turning the rotor capability based on the same supply of electricity power. When the rotor is placed on the edge of the actuator being 90° arc region, the actuator will rotate the rotor in a state of disequilibrium in clockwise or counterclockwise directions, as show in Figure 3. The home position of geometrical positioning mark on rotary platform was never turned back when running the motor ceaselessly in either clockwise or counterclockwise directions by the means of applied periodic sinusoidal command.

This was because of θ_R always being less than θ_F due to the less efficient deformation, resulting in the existence of the escalated slope as show in Figure 3a. And linear increment amount $\theta_F - \theta_R$ for position error obviously is continually multiplied. Therefore, the position trajectory of the USM looks like as raised loops with identical pitches, as show in Figure 3b.

2.2. Dead-zone phenomenon of USM mechanical structure

For PZT thin-disc structure vibration in ultrasonic frequency, PZT plays the driving source to generate the high frequency extended-shrunk motion of metal sheet. The metal sheet plays the amplifier of vibrating magnitude and constructs the desired mode shapes. The minimum deformation located at central portion but larger deflection near outer edge of metal sheet. In contrast, metal stiffness of sheet also constrains the PZT, and limits the PZT dynamic response to electric power. Only in suitable power entry matching resonant frequency and appropriate mechanism configuration for rotor-stator contact, metal stiffness would be overcome by PZT to produce the optimal efficiency. Thus, a PZT actuator is fixed to a normal preload mechanism. The designed preload is conformed that the movable actuator and fixed rotor must contact anytime. Because of the kinetic transformation of resonant deformation on metal sheet by mean of contact force offered by normal preload mechanism, the

effective force will revolve the rotor from the controllable mode shape driving mechanism, especially in ultrasonic frequency. However, there is dead-zone phenomenon due to structure hysteresis and frictional stick-slip circumstance, as shown in Figure 4 described the characteristic curve of rotor speed depending on the applied voltage and driving frequencies. The dead-zone line (a) displays the existence of dead-zone phenomenon under free loading owing to the compound effect of metal deformation and frictional transmission. Because mechanical strength from metal stiffness should be overcome by PZT initially after electrical power input, the actuator always well-being follows the flexural-like vibration of PZT corresponding to voltage oscillation to produce the effective driving force. If it were used as an actuating source but with lower amplitude voltage than ± 3.8 V, the extended-shrunk deformation on metal sheet could not perform well to obtain the efficient mechanical output for rotor turning. Otherwise, when adding external loading onto the platform of USM, dead-zone phenomena in rotational characteristic curve were aggrandized as shown in dead-zone line (b)-(d) of Figure 4. The loading feature depicts that frictional transmission is influenced by the mass inertial of external loading; i.e., larger external loading needs higher input voltage to generate more efficiently deflected force of metal sheet to overcome the static friction between stator and rotor. That is, the system only in operating has input voltage over ± 3.8 V at 67 kHz or 75 kHz under free loading, but also, in loading situation, the system must be boosted up more input power for USM running. For instance, with loading about 1 kg, it needs to directly supply ± 6 V to configure the ultrasonic driving mechanism at least.

And, although the actuator will rotate the rotor in an unequal rotary speed in clockwise (ω_F) or counterclockwise (ω_R), initially, the different ratio in rotary speed has the maximum amount about 1:1.33 of $(\omega_R)_{\max}$ and $(\omega_F)_{\max}$ under free loading. This unbalance rotary speed should cause the serious positioning error if without control system for this novel USM. Fortunately, adding more external loading onto the platform of USM, the same ratio of unbalance rotary speed is almost kept. The worst case of revolution ratio is less than 1:1.30 of ω_R and ω_F with external loading 1050 g, as shown in Figure 4. Thus, this novel USM will offer excellent capability in positioning response.

Hence, the nonlinear behavior of mechanical hysteresis phenomenon of rotation between rotor and stator in (counter-) clockwise, nonlinear kinematical interference from slip-stick transmission in frictional contact, and nonlinear metal deformation by extended-shrunk vibration must be considered as the system parameter of position tracking for the ultrasonic motor. It is necessary to overcome the dead-zone phenomenon of USM's mechanical structure when the system is ignition. Therefore, the advanced modern control strategy of fuzzy sliding-mode design for precise positioning becomes clear subject to confine the dead-zone and hysteresis phenomena in kinetic transfer of the PZT thin-disc USM.

3. The dynamic model of ultrasonic servo drive system

In practical realization of a USM servo control system, it is necessary to represent the dynamic model of the USM mathematically. However, the dynamic model of the USM is extremely difficult to derive from a theoretical point of view because it contains many complicated and nonlinear characteristics which depend on the operating temperature, load torque, applied voltages, and the static pressure force between a stator and a rotor of USMs [2]. By using with the driving circuit, an experimental model of the USM can be established for the purpose of controller design.

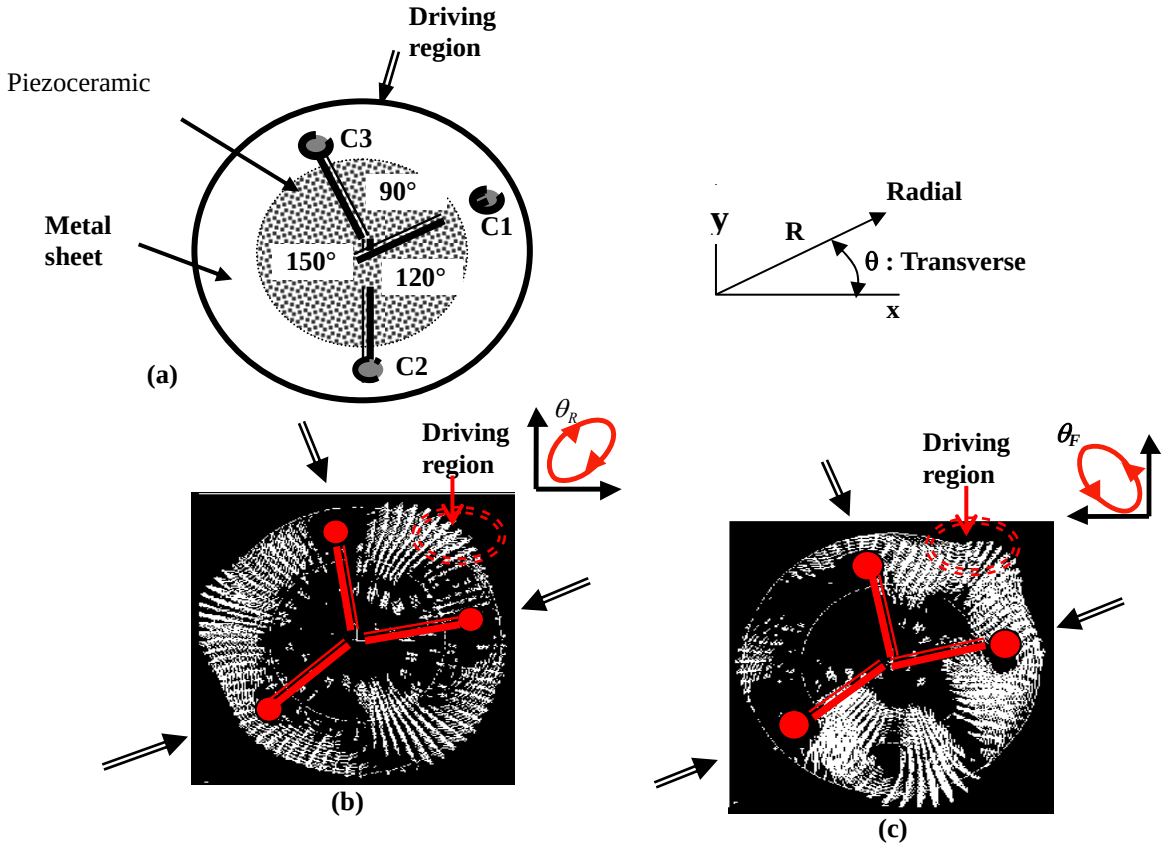

Figure 2. Driving vibration mode (a) scheme with three Constraints placed 90°, 120°, 150° arc location, (b) simulation at 67 kHz, and (c) simulation at 75 kHz Arrows point to the constraint points

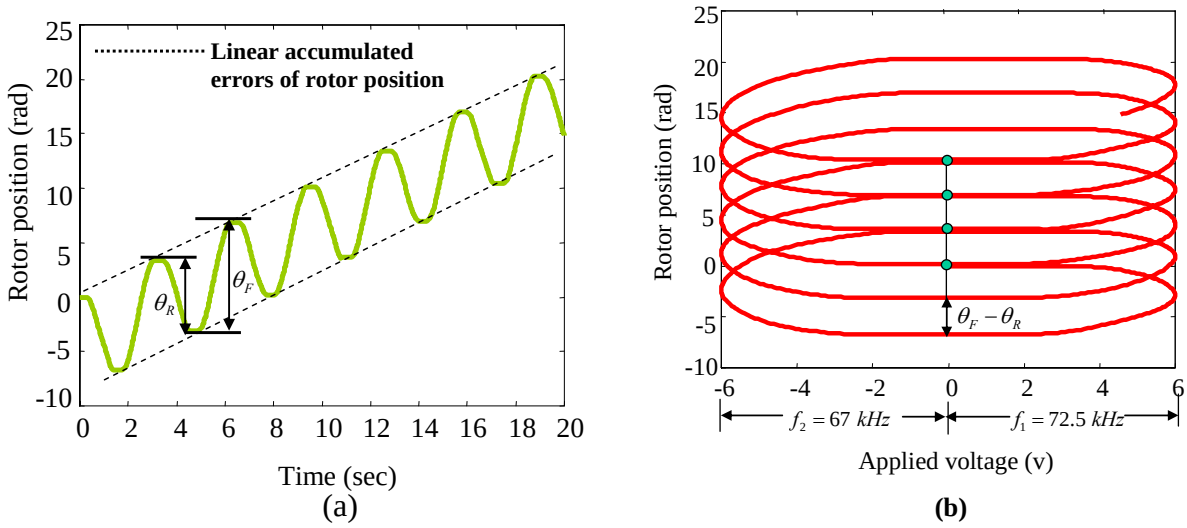

Figure 3. The hysteresis characteristic of rotor position for USM running in clockwise and counterclockwise

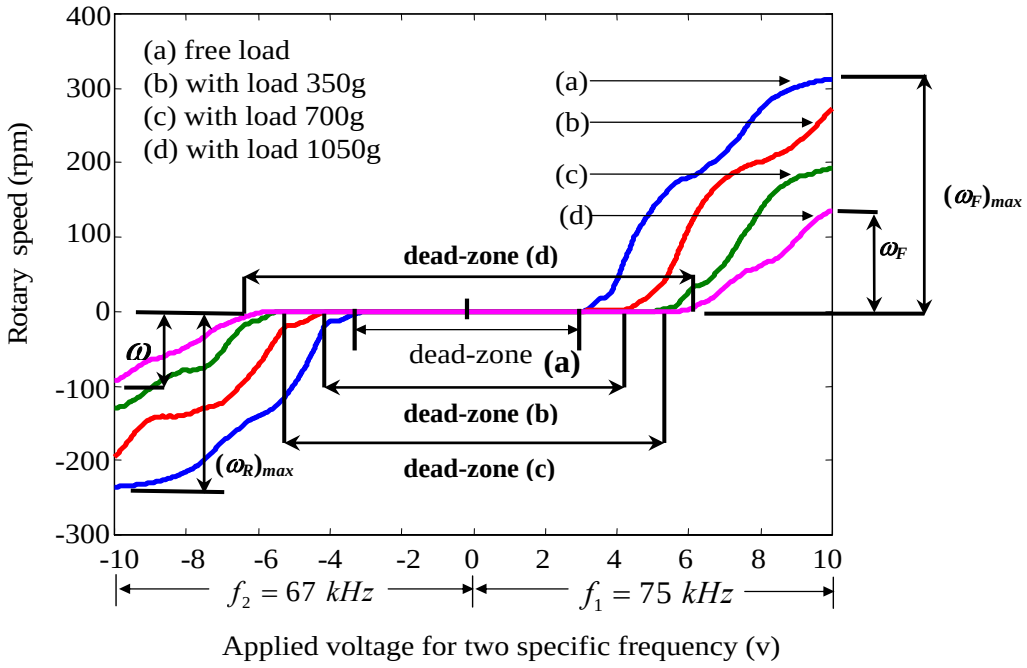

Figure 4. Rotor speed versus applied voltage for two specific frequency of USM

3.1. The driving circuit design

According to ultrasonic modal analysis and actuating characteristic curves of rotary speed and driving frequencies [1, 3], the angle displacement per input signal period was directly determined by the sinusoidal amplitude of the input voltage onto the piezoceramic of an ultrasonic motor. And, the rotary direction was controlled by specific driving frequencies of sinusoidal input voltages.

In order to satisfy the characteristics of frequency control for ultrasonic motor, one set of effective driving circuits was implemented as shown in Figure 5. The major components compose of a bi-quadrant chopper circuit and a single-phase half-bridge series-resonance inverter. The bi-quadrant chopper circuit is a step-down DC/DC power buck converter which higher DC voltage level is transformed to lower DC voltage level. Its adjustment of duty cycle follows the command u_p from controller transferring through D/A servo control card and voltage lever shifter. The buck converter offers a variant DC voltage source $\boldsymbol{V_{dc}}$ as the input of a single-phase half-bridge series-resonance inverter to control the output voltage $\boldsymbol{V_{ac}}$ onto ultrasonic piezoceramics. The driving frequencies of inverter output is chosen by signal u_p via predefined in VCO(1) and VCO(2) of a frequency selector for rotation in clockwise and counterclockwise, respectively. By a voltage control oscillator, When u_p equals to Hi, the frequency f_1 (=75 kHz) is chosen and ultrasonic motor rotates clockwise. In contrast, when u_p is low, the frequency f_2 (=67 kHz) is selected and ultrasonic motor also rotates counterclockwise.

3.2. The approximate dynamic model of USM

As the USM is a highly nonlinear and time varying system, it is difficult to obtain a useful dynamic model for control by mathematical description. Hence, it is practical to obtain the dynamic model experimentally. One set was chosen, under appropriate mechanical design and assembly at suitable driving frequ-

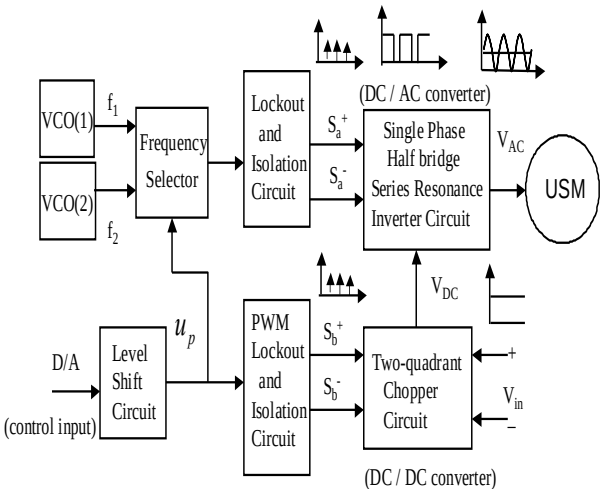

Figure 5. Block diagram of the driving circuit

ncies for the ultrasonic motor, and the open loop off-line system identification method to deal the approximate dynamic model for this study. The relative transfer function was calculated in the arithmetical mean value of rotor speed, divided by input voltage under free and 1 kg weight loading conditions at the specific operating frequency.

For experimental configuration of modeling as shown in Figure 6, the existing icons of white noise mixed sign function in Simulink/Matlab software was applied to construct Pseudo Random Binary Sequence (PRBS).

And, PRBS was transformed as exciting voltage (V) input via D/A converter in the servo control card. The voltage input signal (V) shown in Figure 6a, an exciting energy, stimulated the pizeoceramic ultrasonic motor through driving circuit at specific frequency f_1 and f_2. By mean of the treatment of optic encoder and CPLD module, the response output signal of angular speed (ω) was acquired as shown in Figure 6b. The technique of system identification was proceeded by total 50,000 data in 1 ms sampling interval as modeling database. Then, the first 40,000 data were modeled in white noise model structure of output error (OE) model estimator upon the signals of V and ω to complete the first order parameter identification. The validation of model was recognized by the last 10,000 data, the signal curve of model checked (sampling from 5,000 to 5500 data) as shown in Figure 6c. The approximated transfer function of rotor angular speed to actuator input voltage is $\omega(s)/V(s)=b/(s+a)$. As such, after time integral calculation, the equation represents the approximated transfer function of the rotor position to stator input voltage as $\theta(s)/V(s)=b/[s(s+a)]$,
where

$$a = a_0 \pm \Delta a \ , \ 3.94 \le a \le 10.99$$
$$b = b_0 \pm \Delta b \ , \ 1.932 \le b \le 13.52$$
$$a_0 = 7.465, \ b_0 = 7.726 \ ; \ \Delta a = 3.525, \ \Delta b = 5.794$$

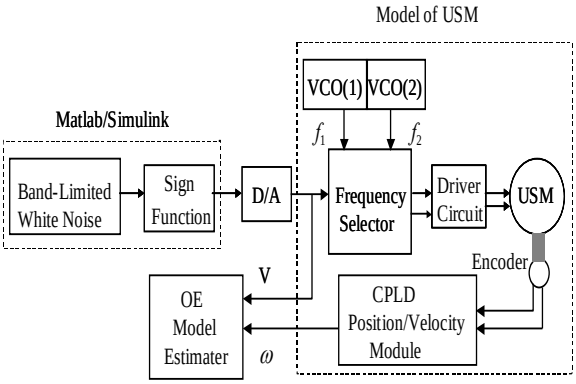

Figure 6. Block diagram of system identification

4. Fuzzy sliding mode controller (FSMC) design

According to system identification, the second order transfer function of the rotor position to input voltage for the USM is represented in the following mathematical model [15],

$$\frac{\theta(s)}{u(s)} = \frac{k_m}{s(1+\tau s)} \qquad (1)$$

Assuming the non-linearity behavior of ultrasonic system as the equivalent disturbance torque, the differential Equation 1 becomes,

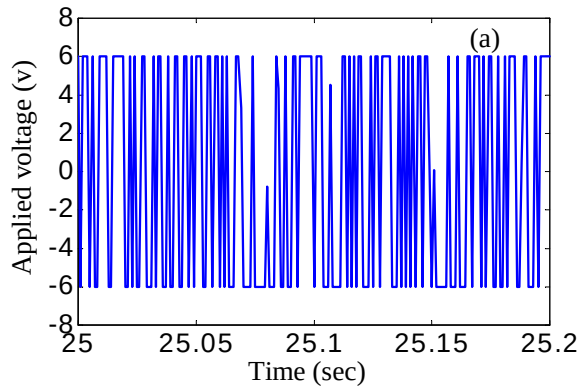

Figure 6a. Input PRBS exciting signal for system identification

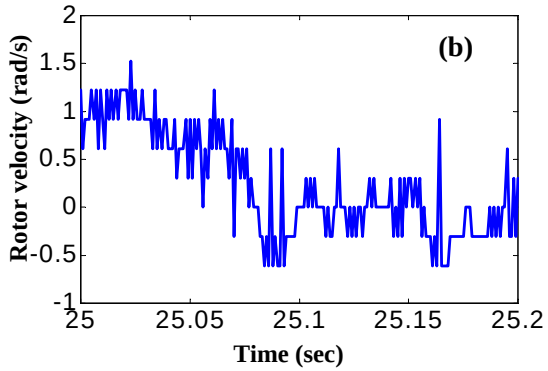

Figure 6b. Rotor velocity signal of USM for system identification

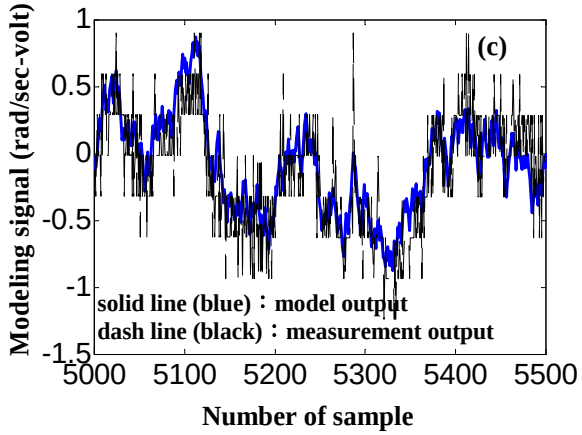

Figure 6c. Signal of modeling validation for system identification

$$\ddot{\theta}(t) = -a_0\dot{\theta}(t) + b_0 u(t) - \frac{1}{J_0}T_d(t) \tag{2}$$
$$T_d(t) = T_L + \Delta J\ddot{\theta}(t) + J_0\Delta a\dot{\theta}(t) - J_0\Delta b u(t)$$

where $T_d(t)$ is an equivalent disturbance torque; $a_0 = 1/\tau$, $b_0 = k_m/\tau$; J_0 and T_L are an equivalent constant for the moment of inertia and the loading torque, respectively. Δa, Δb, and ΔJ are corresponding to the varying amount of normalized system parameters a_0 , b_0 , and J_0 , respectively. All system uncertainty amount, $d(t) = T_d(t) / J_0 b_0$, is also assumed to be bounded as follow,

$$|d(t)| \le k \tag{3}$$

Figure 7 shows the position control system of USM, where $r(t)$ is defined as position command, $x_{1d}(t)$ as desired the position command, and $x_1(t)$ as a real position of the rotor. In order to achieve smoothing position command, the prefilter, the second order function $m(s) = \dfrac{m_2}{s^2 + m_1 s + m_2}$, was employed. And the tracking error is,

$$e(t) = x_1(t) - x_{1d}(t) \tag{4}$$

The system state equation then becomes,

$$\dot{x}(t) = Ax(t) + B(u(t) + d(t)) \; ; \; y(t) = Dx(t) \tag{5}$$

Where $A = \begin{bmatrix} 0 & 1 \\ 0 & -a \end{bmatrix}$, $B = \begin{bmatrix} 0 \\ b \end{bmatrix}$, $D = \begin{bmatrix} 1 & 0 \end{bmatrix}$ (6)

Their variations are caused by the change of mass of the external load, the imprecision of parameters and the external disturbance. According to above mathematical model, the design procedure for sliding-mode controller is described as following.

4.1. Sliding-mode controller design

In the approach of the sliding-mode control (SMC), two or more substructures were created from controlled plant; and some appropriated switching condition was purposely

added to generate the sliding mode action for reaching controllable goals. It is necessary to design a sliding function and next to force system's trajectory into the sliding surface immediately via the control manner. Once the system trajectory slipped into the sliding surface, it was confined. The control action was difficultly further away when external interference was occurred.

Even though the position tracking error was taken place due to variation of external loading or internal parameter, the system stability was guaranteed if that uncertain amount was allowed in the design specification. When position tracking error appears, system trajectory was only restricted in $s(t) = 0$ tiny space near sliding surface to do extra high frequency crash motion until the control target is reached if the uncertain amount within design range.

That is, system trajectory has excellent robust ability in noise rejection. In order to guarantee the existence of approaching mode and sliding mode in the system, design stages are described as the following section.

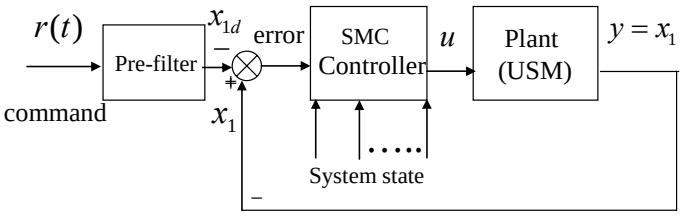

Figure 7. Block diagram of USM position control system using SMC

4.1.1. Sliding function design

In order to stabilize the system tracking path approaching the control target in sliding mode, it is necessary to select the appropriate integral form of switching function as follows,

$$s(t) = \dot{e}(t) + c_1 e(t) + c_2 \nu \tag{7}$$

$$\nu = \int_0^t e(\tau)\, d\tau \tag{8}$$

where ν is an integration term to reduce the system's steady state error. The positive coefficients of c_1 and c_2 are assigned to gain the negative real roots of system dynamic characteristic equation desirably. If the system was located at sliding mode, then $\dot{s}(t) = s(t) = 0$, system trajectory could approach the control target. Finally, the system tracking error gradually was converged into zero.

4.1.2. SMC position controller design

To assure that the system approaches the sliding surface in limited time and that the sliding mode behavior exists, the position controller is designed as the follows,

$$u(t) = u_{eq}(t) + u_{sw}(t) \tag{9}$$

$$\begin{aligned} u_{eq}(t) = b_0^{-1}[&-c_2 x_1(t) + (a_0 - c_1)x_2(t) + m_2 r(t) \\ &+ (c_2 - m_2)x_{1d}(t) + (c_1 - m_1)\dot{x}_{1d}(t)] \end{aligned} \tag{10}$$

$$u_{sw}(t) = -(k + \sigma)\, sign(s(t)) \tag{11}$$

Where $\sigma > 0$, is the speed of approaching sliding mode, $u_{eq}(t)$ is the input term of equivalent control, $u_{sw}(t)$ is the input term of discontinuously switching control; $sign(\bullet)$ is a sign function that is an ideal switching function defined as follow,

$$sign(s(t)) = \begin{cases} +1 \ , \text{ if } s(t) > 0 \\ -1 \ , \text{ if } s(t) < 0 \end{cases} \tag{12}$$

and where k is a positive value defined as $|\, d(t)\, | \le k$.

Lemma: If the sliding function s(t) of control system satisfied the following conditions, then the existing condition of guaranteed approaching and sliding mode behavior would be sustained [16].

$$\lim s(t)\dot{s}(t) \le -\sigma |s(t)| \ ; \ \sigma > 0 \ , \ s(t) \ne 0 \tag{13}$$

Proof : according to lemma, then

$$
\begin{aligned}
&s(t)\dot{s}(t) = s(t)\{\ddot{e}(t) + c_1\dot{e}(t) + c_2 e(t)\} \\
&= s(t)\{(\ddot{x}_1(t) - \ddot{x}_{1d}(t)) + c_1(\dot{x}_1 - \dot{x}_{1d}) + c_2(x_1 - x_{1d})\} \\
&= s(t)\{(-ax_2(t) + b(u(t) + d(t)) - m_2 r(t) + m_1\dot{x}_{1d}(t) \\
&+ m_2 x_{1d}(t)) + c_1(x_2(t) - \dot{x}_{1d}(t)) + c_2(x_1(t) - x_{1d}(t)) \\
&= s(t)\{c_2 x_1(t) + (c_1 - a)x_2(t) - m_2 r(t) + b(u(t) + d(t)) + \\
&\quad (m_2 - c_2)x_{1d}(t) + (m_1 - c_1)\dot{x}_{1d}(t)\} \\
&= s(t)\{c_2 x_1(t) + (c_1 - (a_0 + \Delta a))x_2(t) - m_2 r(t) + (b_0 + \Delta b) \\
&[b_0^{-1}(-c_2 x_1(t) + (a_0 - c_1)x_2(t) + m_2 r(t) + (c_2 - m_2)x_{1d}(t) \\
&+ (c_1 - m_1)\dot{x}_{1d}(t)) - (k + \sigma)sign(s(t)) + d(t)] \\
&+ (m_2 - c_2)x_{1d}(t) + (m_1 - c_1)\dot{x}_{1d}(t)\} \\
&= s(t)\{-\Delta a \cdot x_2(t) + \Delta b \cdot b_0^{-1}(-c_2 x_1(t) + (a_0 - c_1)x_2(t) \\
&+ m_2 r(t) + (c_2 - m_2)x_{1d}(t) + (c_1 - m_1)\dot{x}_{1d}(t) \\
&- (k + \sigma)sign(s(t)) + d(t)\} \\
&= s(t)\{-\frac{\Delta b \cdot c_2}{b_0}x_1(t) + (\frac{\Delta b}{b_0}(a_0 - c_1) - \Delta a)x_2(t) + \frac{\Delta b \cdot m_2}{b_0}r(t) \\
&+ \frac{\Delta b(c_2 - m_2)}{b_0}x_{1d}(t) + \frac{\Delta b(c_1 - m_1)}{b_0}\dot{x}_{1d}(t) \\
&- (k + \sigma)sign(s(t)) + d(t)\} \\
&\le s(t)\{E(t) - (k + \sigma)sign(s(t))\} \\
&\le -\sigma|s(t)| - k|s(t)| + |s(t)|E(t) \\
&= -\sigma|s(t)| - k|s(t)|[1 - \frac{E(t)}{k}] \\
&\le -\sigma|s(t)| \qquad (14)
\end{aligned}
$$

$$
\begin{aligned}
E(t) = &\left|\frac{\Delta b \cdot c_2}{b_0}x_1(t)\right| + \left|(\frac{\Delta b(a_0 - c_1)}{b_0} - \Delta a)x_2(t)\right| + \left|\frac{\Delta b \cdot m_2}{b_0}r(t)\right| \\
&+ \left|\frac{\Delta b(c_2 - m_2)}{b_0}x_{1d}(t)\right| + \left|\frac{\Delta b(c_1 - m_1)}{b_0}\dot{x}_{1d}(t)\right| + |d(t)| \qquad (15)
\end{aligned}
$$

Therefore, only if $k \ge E(t)$ existed in Equation 14, the existing condition of approaching and sliding mode behaviors in lemma would be satisfied by the SMC position controller using Equation 9. System state *x(t)* shall steadily slide to control target along sliding surface. In order to prevent the non-interrupt chattering phenomena in tiny space near the sliding mode *s(t)* = 0 of the system tracking path and unexpected high frequency noise, sliding bounded layer concept promoted by Slotine et al. [11, 16] that is, sign(s) was inferior to sat(s, ε). The function of $sat(s,\varepsilon)$ is defined as follows:

$$
sat(s,\varepsilon) = \begin{cases} 1 \;;\; s > \varepsilon \\ s/\varepsilon \;;\; |s| \le \varepsilon \\ -1 \;;\; s < -\varepsilon \end{cases} = \begin{cases} sign(s) \;;\; |s| > \varepsilon \\ s/\varepsilon \;;\; |s| \le \varepsilon \end{cases} \qquad (16)
$$

where ε is bounded layer that is infinitsmal positive. For a system reaching the control target quickly, the corrective term $\alpha \cdot s(t)$ was subjoined into the control rule. Hence, the modified control rule is:

$$
\begin{aligned}
u(t) = &b_0^{-1}[-c_2 x_1(t) + (a_0 - c_1)x_2(t) + m_2 r(t) + \\
&(c_2 - m_2)x_{1d}(t) + (c_1 - m_1)\dot{x}_{1d}(t)] \\
&- (k + \sigma)sat(s(t), \varepsilon) + \alpha \cdot s(t)) \qquad (17)
\end{aligned}
$$

4.2. Fuzzy sliding-mode controller design

SMC has excellent robust ability in noise rejection only when system trajectory being within sliding mode. While a system in approaching mode, it is very sensitive to uncertain parameters and noise disturbance for the system dynamic behavior. Therefore it is necessary to recognize the upper bound of uncertain amount for the SMC design in order to guarantee the existence of the approaching mode and the sliding mode in the system.

The control input term u_{sw} of Equation 11 was applied to suppress uncertain amount in system, but the determination of *k* value was difficult. If *k* value is too much, it will lead control input onto extremely chattering phenomena. If *k* value is too less, probably the system will be unstable. Thus, in this study, the inference mechanism of fuzzy control theory was employed to deal with k_f rather than *k* value [17, 18]. The design stages of fuzzy sliding mode control (FSMC) are de-

scribed as the follow,

$$u(t) = u_{eq}(t) + u_{sw}(t) \tag{18}$$

$$u_{eq}(t) = b_0^{-1}[-c_2 x_1(t) + (a_0 - c_1)x_2(t) + m_2 r(t) + (c_2 - m_2)x_{1d}(t) + (c_1 - m_1)\dot{x}_{1d}(t)] \tag{19}$$

$$u_{sw}(t) = -k_f sign(s(t)) \tag{20}$$

where k_f was estimated via reasoning from fuzzy control, as shown in Figure 8 illustrated the block diagram of USM position control system using FSMC. Assigned $s(t)$ and $s(t)\dot{s}(t)$ as input variables and k_f as a output variable, k_s and $k_{s\dot{s}}$ are input quantitative factors and $k_{\Delta K}$ is an output quantitative factor, respectively, i.e.

$$s_f = s \times k_s \quad ; \quad s\dot{s}_f = s\dot{s} \times k_{s\dot{s}} \quad ; \quad k_f = \Delta k_f \times k_{\Delta k}$$

It is a very important term of $k_{\Delta k}$ assignment. If k_f was a relative large positive value, there was an extra high frequency chattering phenomenon occurred in the system. In contrast to, assuming a relative less negative k_f value, the system trajectory will be further away the sliding surface, or the worst case is never reaching the sliding surface. Therefore, the design of $k_{\Delta k}$ should be considerably careful. Here, linguistic variables of fuzzy logic set are defined as,

N：negative ; ZO：zero ; P：positive
NB：negative big ; NM：negative medium
NS：negative small ; PS：positive small
PM：positive medium ; PB：positive big

Corresponding membership functions of μ_{S_f}, $\mu_{S\dot{S}_f}$, and $\mu_{\Delta K_f}$ and their features are defined as shown in Figure 9.

From the derivation of equation (14) known, the value of k_f would be too small if $s(t)\dot{s}(t)$ was positive so that the influence of term of $E(t)$ could not overcome and system trajectory would be further away $s(t) = 0$ Therefore, in this situation, the value of k_f should be increased to positive gradually. In contrast to, if $s(t)\dot{s}(t)$ was negative, the approaching mode was satisfied so that the system motion trajectory would move more closer to $s(t) = 0$.

However, in this case, the control input obviously became greater resulting in surplus control. Therefore, to avoid undesired surplus control, the value of k_f should be modified to negative gradually. But the negative value of k_f should not be too less so that the system would be further away $s(t) = 0$ again.

In order to guarantee the whole motion trend towards $s(t) = 0$, we design the membership of the output signal as shown in Figure 9c. Especially, in the case of $s(t)\dot{s}(t) = 0$ and $s(t) \neq 0$, the value of k_f should be increased for the system trajectory approaching $s(t) = 0$. For accomplishing above fuzzy reasoning, the fuzzy logic rule tables in different status are shown in Table 1 and Table 2.

The fuzzy logic knowledge base consists of a set of fuzzy IF (a set of conditions are satisfied) THEN (a set of consequence can be inferred) rules which themselves consist of a set of linguistic variables associated with inputs and outputs and fuzzy operators such as AND and OR. For instance, in the case of a two –input –single output (MISO) fuzzy system, fuzzy control rules have the following form:

$$R_i : \text{IF } \hat{x} \text{ is } A_i \text{ and } \hat{y} \text{ is } B_i \text{ THEN } \hat{z} \text{ is } Z_i \tag{21}$$

where $\hat{x}$, $\hat{y}$, and $\hat{z}$ are linguistic variables respecting two process state variables and one control variable. A_i, B_i, and $Z_i (i = 1, 2, ..., n)$ are values of the linguistic variables $\hat{x}$, $\hat{y}$, and $\hat{z}$ in the universe of discourse U, V, and W, respectively. The fuzzy implication rule of Mamdani's min-min-max method is used for fuzzy reasoning and its algorithm is Equation 22 as,

$$\mu_C(w) = \bigvee_{i=1}^{n} \alpha_i \wedge \mu_{C_i}(w) \equiv \bigvee_{i=1}^{n} \left[\mu_{A_i}(x_0) \wedge \mu_{B_i}(y_0)\right] \wedge \mu_{C_i}(w) \tag{22}$$
$$= [\alpha_1 \wedge \mu_{C_1}(w)] \vee [\alpha_2 \wedge \mu_{C_2}(w)] \vee \cdots \vee [\alpha_n \wedge \mu_{C_n}(w)]$$

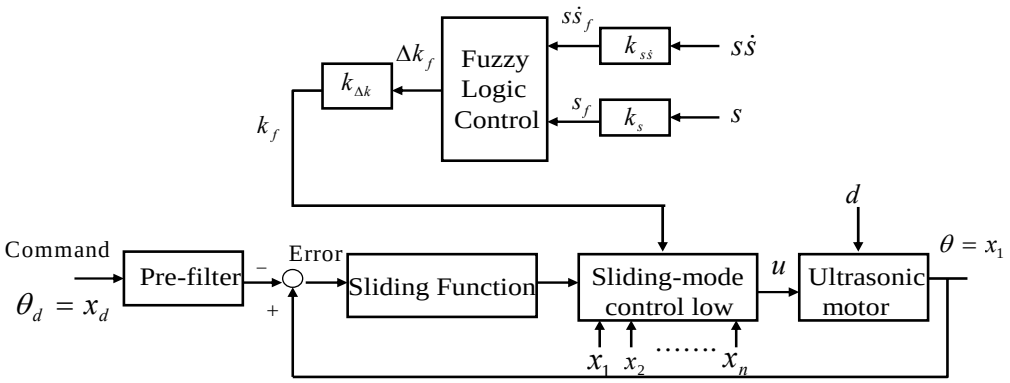

Figure 8. Block diagram of USM position control system using FSMC

Table 1. Fuzzy rule base for $s\dot{s} \neq 0$

$s\dot{s}_f$	NB	NM	NS	PS	PM	PB
Δk_f	NB	NM	NS	PS	PM	PB

Table 2. Fuzzy rule base for $s\dot{s} = 0$

s_f	NB	NS	ZO	PS	PB
Δk_f	PS	PS	ZO	PS	PS

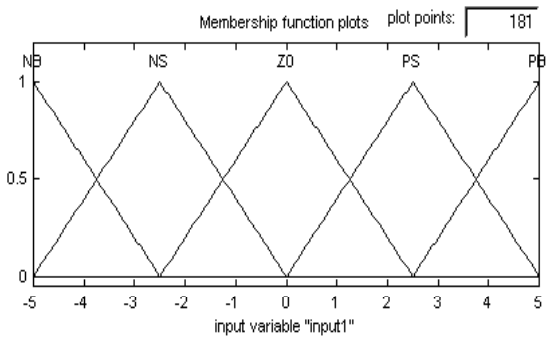

(a) μ_{S_f}

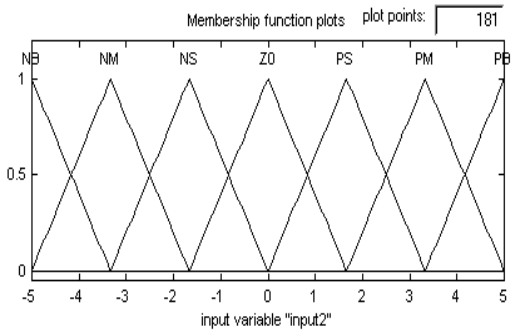

(b) $\mu_{s\dot{s}_f}$

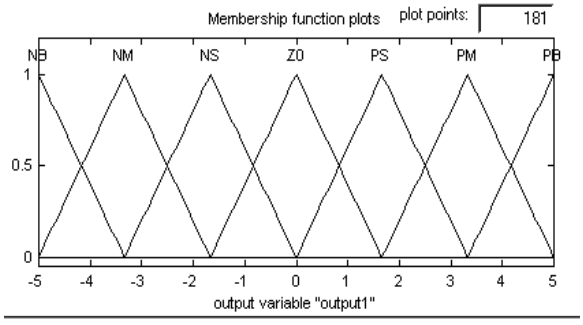

(c) $\mu_{\Delta k_f}$

Figure 9. Membership function for $(a)\mu_{S_f}$, $(b)\mu_{S\dot{S}_f}$, *and* $(c)\mu_{\Delta K_f}$

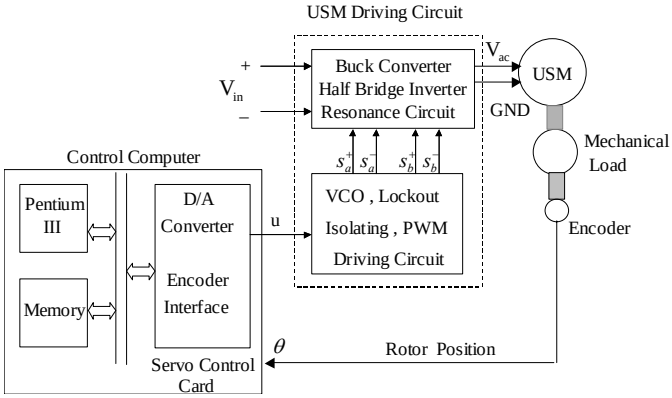

Figure 10. PC-based USM driving circuit and control system

where the firing strength α_i is a measure of the contribution of the ith rule to the fuzzy control action.

The output k_f of fuzzy inference was calculated in defuzzification by mean of the center of gravity method of equation (23),

$$k_f = \frac{\sum_{i=1}^{11} W_i B_i}{\sum_{i=1}^{11} W_i} \tag{23}$$

where $W_i = [\mu_{A_i}(x_0) \wedge \mu_{B_i}(y_0)]$ is the proper level of preliminary term in i th control rule, B_i is the center value relative to the membership function of the reasoning part in i th control rule.

5. Experimental results and discussion

Figure 10 illustrates the experimental PC-based USM driving control system. The servo control card slotted in PC computer includes multi-channel of A/D, D/A, PIO and optic encoder interface circuits. The output signal of the optic encoder of model MES-30-2000PE is a square signal with A and B phase in 2000 pulse per revolution. The configuration and implementation are set up at Real-Time workshop (RTW) toolbox of MATLAB/SIMULINK software, with 1 ms sampling interval.

For performance evaluation of controllers, utilized the sinusoidal and periodic step signals are as the inputs for position tracking commands through the pre-filter that is a second order transfer function. When the control command was sinusoidal signal, the parameter of the pre-filter was set to 1. If it was set as periodical square signal, the pre-filter would be the transfer function of $\xi = 1, \omega_n = 10$ as the following,

$$\frac{m_2}{s^2 + m_1 s + m_2} = \frac{\omega^2{}_n}{s^2 + 2\xi\omega_n s + \omega^2{}_n} = \frac{100}{s^2 + 20s + 100} \tag{24}$$

In control system design, the characteristic roots of system shall be placed in LHP during the sliding mode, and the system trajectory being along sliding surface. The control target will be gradually reached. Supposing that the placement of dual characteristic roots in the design of a close loop system is located in (-20, 0) of a complex plane, $(c_1\ ;\ c_2)$ of the switching function $s(t)$ in Equation 7 are equal to (40,400). The parameter $(k, \sigma, \alpha, \varepsilon)$ of the controller $u(t)$ in Equation 12 is (20,20, 20, 0.001), and the designed control input of SMC shall be

$$u(t) = 0.13 \cdot [-400x_1(t) + 32.54x_2(t) + 100r(t) + 300x_{1d}(t) + 20\dot{x}_{1d}(t)] - (40sat(s(t), 0.001) + 20s(t)) \tag{25}$$

The experimental analysis was free loading and 1 kg loading, respectively, onto carrying platform of ultrasonic motor testing bench using both scheme of SMC and FSMC. The ex-perimental results shown in Figure 11 and Figure 12, respectively, based on the sinusoid-al command, are addressed in the SMC and FSMC, for the position command tracking.

The step response of the rotor position, tracking error, and control effort using the SMC and FSMC controller are shown in Figure 13 and Figure 14.

According to the experiments shown in Figure 11 and Figure 12, known in sinusoidal

command with both conditions of free and 1 kg loading, the steady error of rotor trajectory was quiet miniature about 0.01 ~ 0.02 radius, when SMC and FSMC method were employed respectively. Their position tracking capability is sufficient for the novel USM.

However, the SMC method has obvious tendency to larger control input and higher chattering phenomena than that of the FSMC method. Furthermore, in the cases of the periodic step command as shown in Figure 13 and Figure 14, the tracking ability was stilled excellent either free loading or 1 kg loading under the SMC and FSMC method. Their tracking error is less than 0.01 ~ 0.02 radius.

However, by using the SMC method, the control input and chattering phenomena were seriously affected by either free loading or external 1 kg weight loading. Based on the above mentioned experimental results, the external loading analysis of tracking errors in the sinusoidal and periodical step command, the error amount of both SMC and FSMC controllers is quite close to that of free loading.

That is, both of SMC and FSMC controllers have efficient performance to over come the non-linear phenomena such as dead-zone and hysteresis behaviors for this USM. And, system uncertainties and external disturbance in SMC and FSMC could be overall insensitive.

As such, the robust performance in noise rejection can be guaranteed. Unfortunately, there always are the more high -frequency chattering phenomena in the SMC system because the discontinuously switching input term u_{sw} of the control command was setting as the constant gain k. In the FSMC system, the input term u_{sw} has the inference mechanism of fuzzy theory in term of k_f so that the dynamic behaviors of control inputs fellow the amount of tracking errors and high-frequency chattering phenomena will be improved. Therefore, FSMC has a small amount of control inputs and chattering phenomena.

6. Conclusion

In the conventional ultrasonic motor, two-phase AC power with high amplitude pulse is applied to generate the traveling waves. However, in the study a single-phase AC power with low voltage at the specific frequency from the driving circuit is employed to complete the position tracking in clockwise and counterclockwise rotations based on the control of SMC and FSMC for the thin-disc PZT driving USM. The mechanical nonlinear being achieved is inherently the hysteresis behavior due to the different deflection of metal sheet and driving frequency, and the dead-zone phenomenon from contact friction and stick-slip motion.

These nonlinear behaviors must be considered in controller design for a preferred efficiency in USM operating. The partial proof in theoretical method has been approached in the control design for robustness in noise rejection, but the full theoretical demonstration to overcome the nonlinear phenomena of the thin-disc USM still needs the further study in the future. Using the approximate mathematical model of transfer function via system identification technique, the performance of SMC and FSMC scheme were evaluated in term of the position tracking command of sinusoidal and step functions.

The experimental results proved that the robust control and low tracking errors could be obtained by both of controllers for the thin-disc USM. But, the superior quality of the FSMC scheme is more suitably applied to the control of this innovative ultrasonic servomechanism in noise rejection without the high frequency chattering phenomena. Also, less control input was needed.

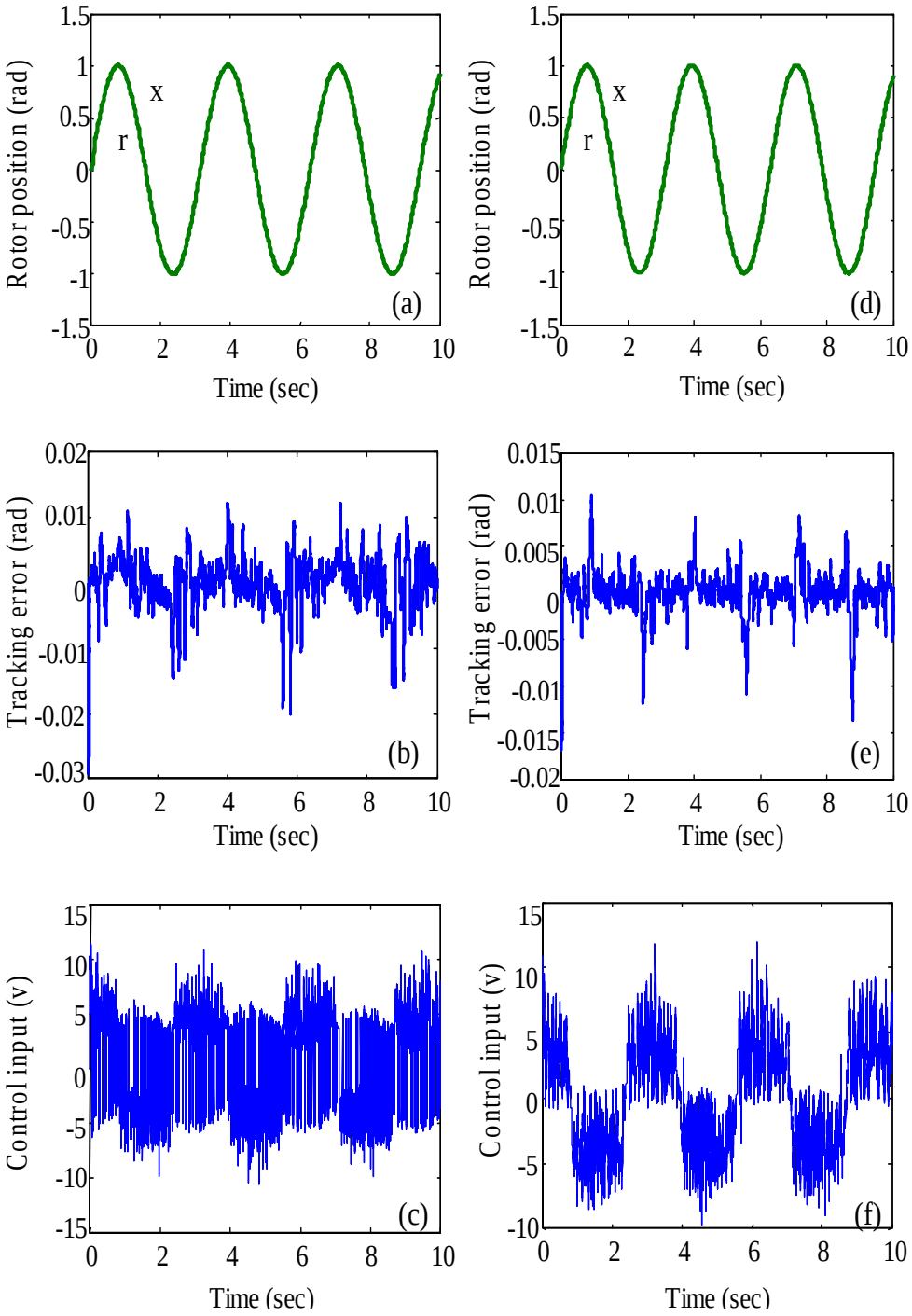

Figure. 11. The experimental results with sinusoidal command (free loading)：(a), (b), and (c) are rotor position, tracking error, and control input of SMC；(d), (e), and (f) are rotor position, tracking error, and control input of FSMC [r = command；x = rotor position]

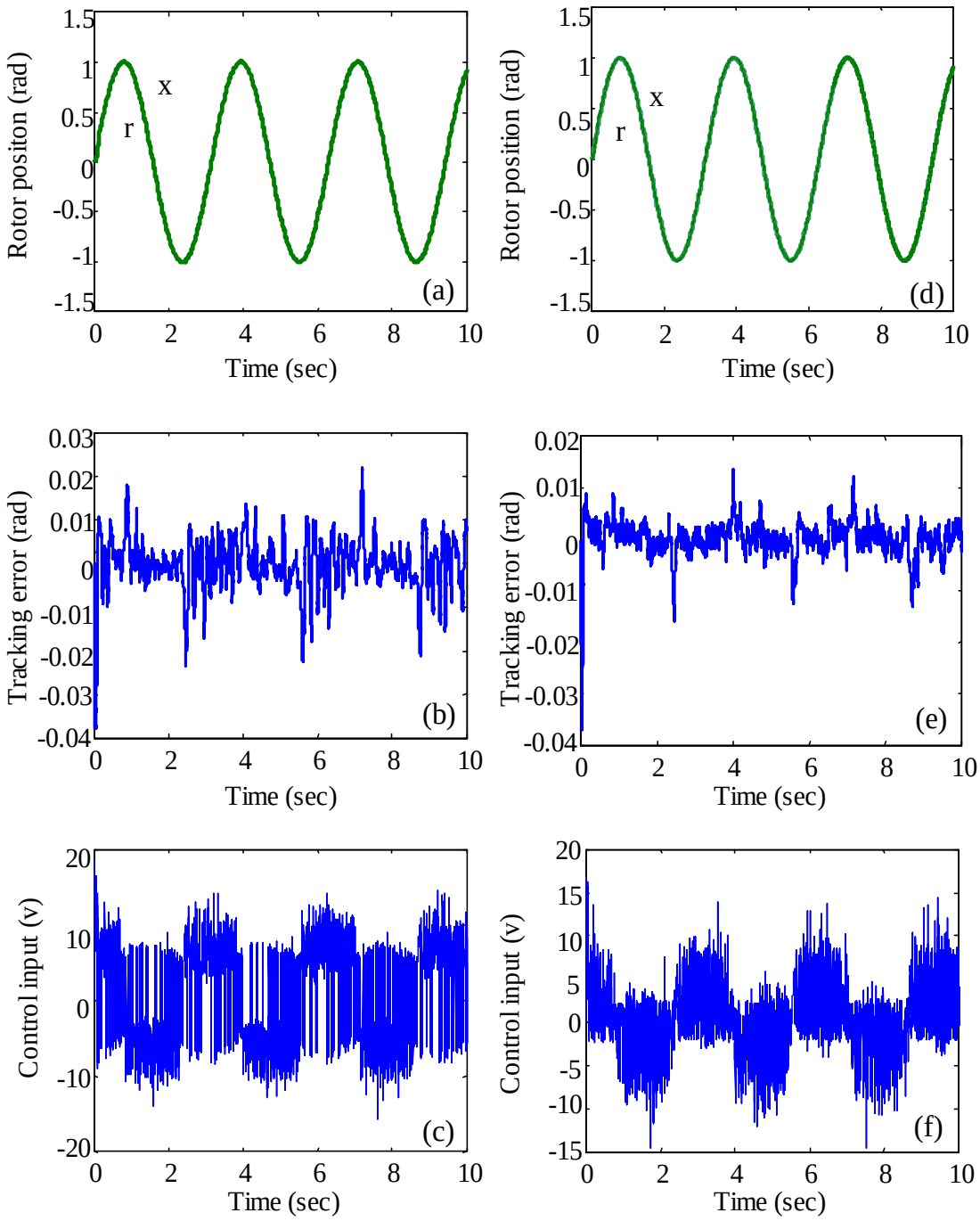

Figure 12. The experimental results with sinusoidal command (1 kg weight loading)：(a), (b), and (c) are rotor position, tracking error, and control input of SMC；(d), (e), and (f) are rotor position, tracking error, and control input of FSMC [r = command；x = rotor position]

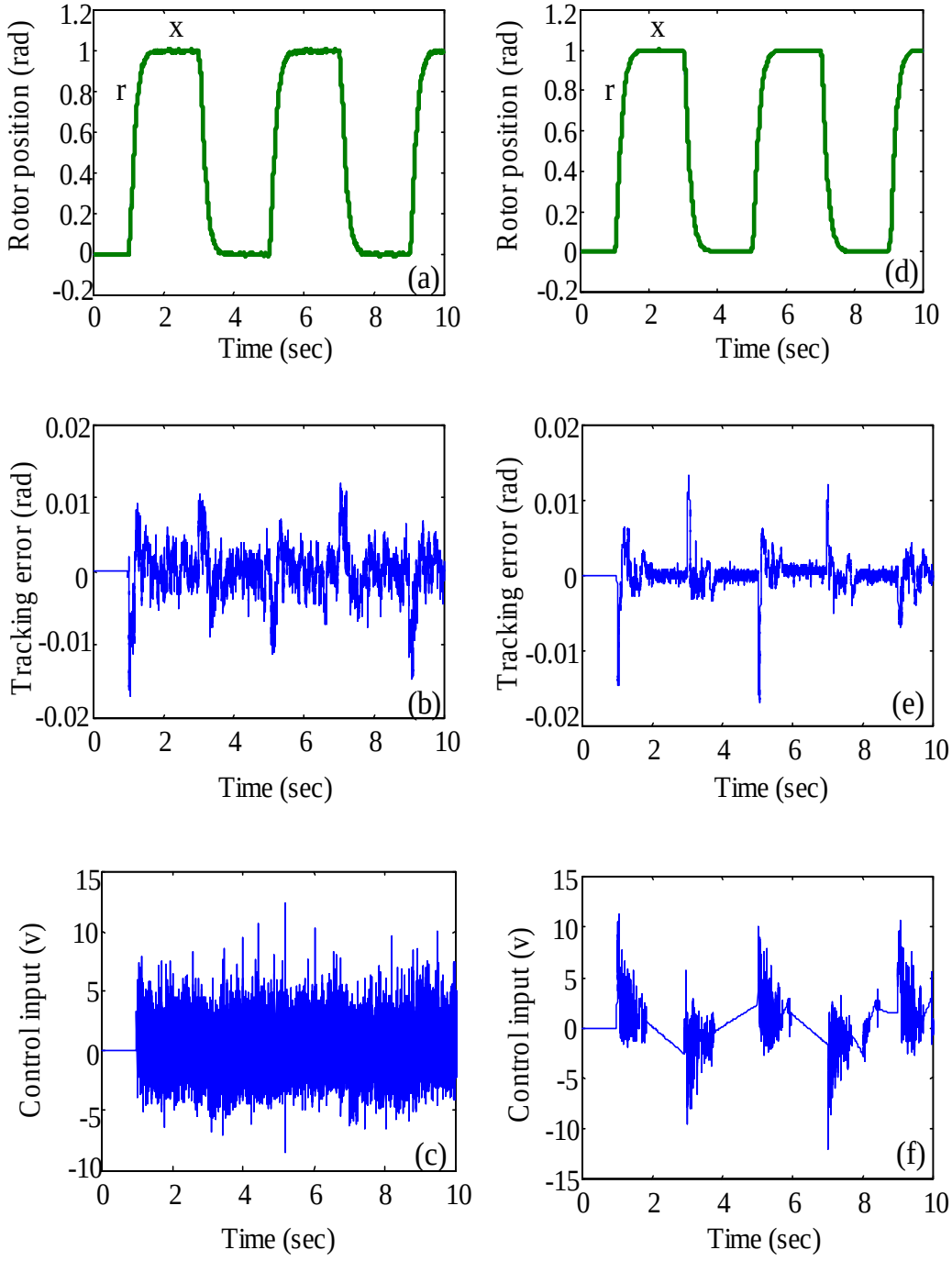

Figure 13. The experimental with periodic step command (free loading)：(a), (b), and (c) are rotor position, tracking error, and control input of SMC；(d), (e), and (f) are rotor position, tracking error, and control input of FSMC [r = command；x = rotor position]

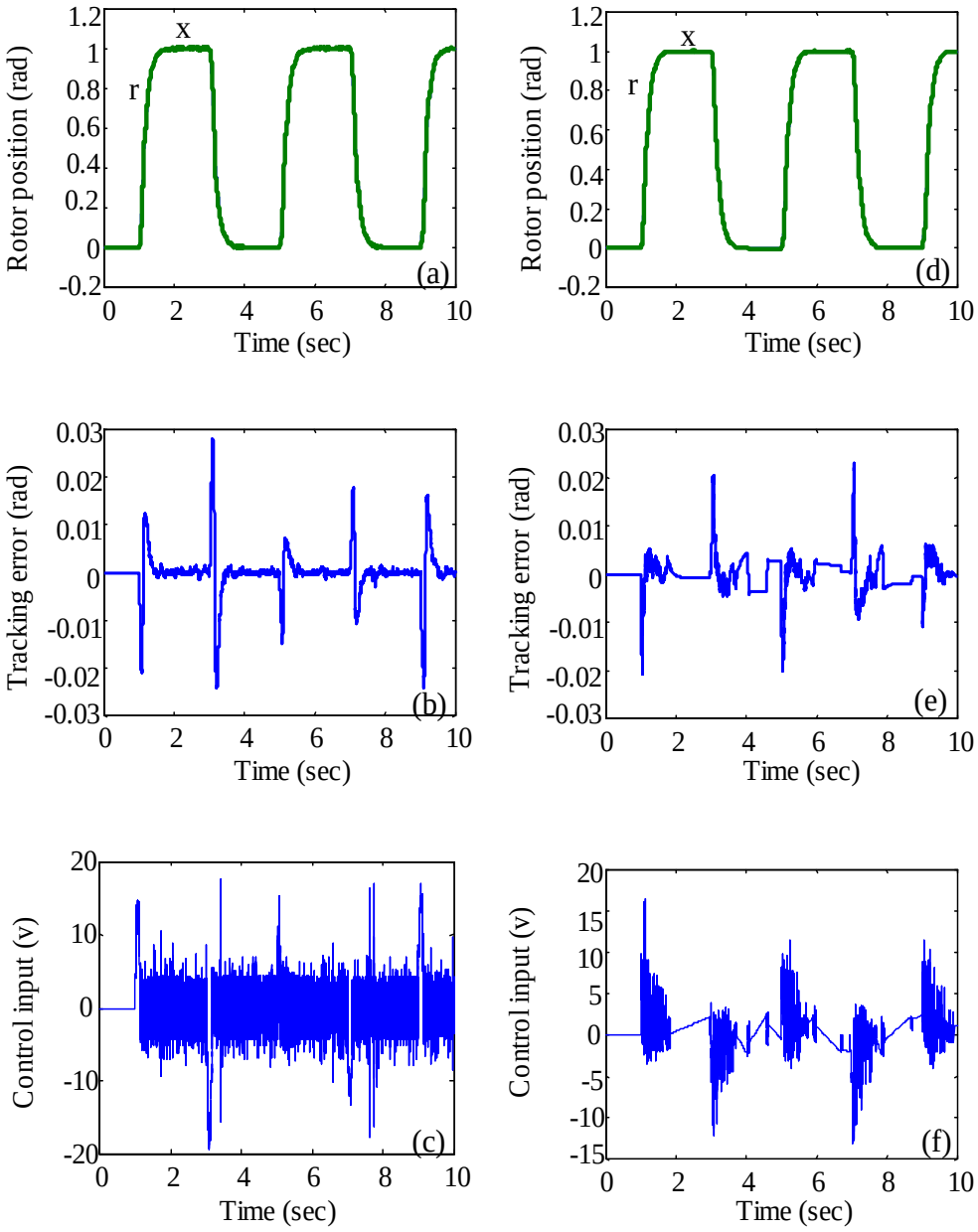

Figure 14. The experimental with periodic step command (1 kg weight loading)：(a), (b), and (c) are rotor position, tracking error, and control input of SMC；(d), (e), and (f) are rotor position, tracking error, and control input of FSMC [r = command；x = rotor position]

References

[1] Wen, F. L., Yen, C. Y., and Ouyang, M. S.2003. Thin-disk piezoceramic ultrasonic motor. Part I: *design and performance evaluation.* Ultrasonics, 41: 437-450.

[2] Yen, C. Y., Wen F. L., and Ouyang, M. S.2003. Thin-disc piezoceramic ultrasonic motor. Part II: *system construction and control*. Ultrasonics, 41: 451-463.

[3] Ouyang, M. S. and Wen, F. L. 2002. Thin-disc Piezoelectric Actuating Ultrasonic Motor. USA Patent: 6 489 705.

[4] Song, G., Chaudhry V, and Batur, C. 2003. Precision tracking control of shape memory alloy actuators using neural networks and a sliding-mode based robust controller. *Smart Material and Structure*, 12: 223-231.

[5] Ge, P. and Jouaneh, M. 1995. Modelinghysteresis in piezoceramic actuators. *Precision Engineering,* 17: 211-21.

[6] Richard, T. and Detournay E. 2000. Stick–slip motion in a friction oscillator with normal and tangential mode coupling. *Friction, Adhesion, Lubrification :*671-678.

[7] Choi, S. B., Kim, H. K., Lim, S. C., and Park, Y. P. 2001. Position tracking control of an optical pick-up device using piezoceramic actuator. *Mechatronics,* 11: 691-705.

[8] Yu, Y., Naganathan, N., and Dukipati, R. 2002. Preisach modeling of hysteresis for piezoceramic actuator system. *Mechanism and Machine Theory,* 37: 49-59.

[9] Yu, Y., Xiao, Z., Naganathan, N. G., an-Dukipati, R. V. 2002. Dynamic preisach modelling of hysteresis for the piezoceramic actuator system. *Mechanism and Machine Theory,* 37: 75-89.

[10] Young, K. D. 1986. A variable structuremodel following control design for robotics applications. *IEEE International Conference Robotics Automation,* San Francisco, CA., U.S.A.: 540-543.

[11] Slotine, J. E. and Sastry, S. S. 1986. Tracking control of nonlinear system using sliding surface with application to robot manipulator,. *International Journal Control,* 38**:** 465-492.

[12] Utkin, V. I. 1993. Sliding mode controldesign principles and applications to electric drives. *IEEE Transaction Industrial Electrons*, 40: 23-36.

[13] Buja, G. S., Menis, R., and Valla, M. I. 1993. Variable structure control of an SRM drive. *IEEE Transaction Industrial Electrons ,* 40: 56-63.

[14] Hashimoto, H., Yamamoto, H., Yana gisava, S., and Harashima, H. 1986. Brushless servomotor control using variable structure approach. *IEEE Industrial Application Society Annu. Meet. Pt.1*: 72-79.

[15] Senjyu, T., Yokoda, S., and Uezato, K. 1998. Position control of ultrasonic motors using sliding mode control with multiple control inputs. *IEEE Ultrasonics Symposium,* 597-602.

[16] Itkis, U. 1976. *Control Systems of Variable Structure*. John Wiely. New York.

[17] Kaiyu, Z., Hongye, S., Jian, C., and Keqin, Z. 2000. Globally stable robust tracking of uncertain systems via fuzzy integral sliding mode control. *IEEE Proceeding of the 3rd World Congress on Intelligent Control and Automation,* P. R. China: 1827-1831.

[18] Lin, F. J. and Chiu, S. L. 1998. Adaptive fuzzy sliding-mode controller for PM synchronous servo motor drives. *IEE Proc. Control Theory Application,* 145: 63-72.